Particle acceleration by magnetic field-aligned electric fields in active galactic nuclei

H. Lesch and G.T. Birk

Institut für Astronomie und Astrophysik der Universität München, Scheinerstrasse 1, D-81679 München, Germany

Abstract. We show that the formation of magnetic field-aligned electric fields $E_\parallel$ explains the existence of relativistic leptons with Lorentz factors less than about 2000 in active galactic nuclei. This Lorentz factor is the minimum value for Fermi processes to accelerate leptons. This is also known as the *injection problem*: particles with $\gamma < 2000$ cannot be accelerated by shock waves or MHD turbulence, also known as Fermi I and II mechanisms. $E_\parallel$ can accelerate charged particles very efficiently on very short time scales. The appearance of such magnetic field-aligned electric fields is an implicit property of magnetized, turbulent plasmas in which the electrical conductivity is not infinitely high. We describe the appearance of these fields within an analytical kinematic approach as well as on the grounds of a numerical dynamical model. Due to the small spatial extension of such layers the acceleration time is much shorter than the energy loss time due to inverse Compton scattering of the UV radiation of the underlying accretion disk. Thus, relativistic leptons can be effectively produced in the corona of an accretion disk even in the presence of an intense radiation bath. This is an important result for γ-ray models, which require a high initial density of leptons with Lorentz factors of about 10^3.

Key words: magnetohydrodynamics – particle acceleration

1. Introduction

There is general consensus that active galactic nuclei (AGN) consist of accreting supermassive black holes (BH) (up to 10^{10} M$_\odot$) surrounded by accretion disks. The disk consists of thermal plasma which is heated via viscous accretion up to temperatures of about $5 \cdot 10^4$ K. The existence of thermal plasma in this temperature range has been established beyond any doubt by optical observations which exhibit line widths up to $3 \cdot 10^4$ km s^{-1} and by UV observations which clearly show spectra compatible with the thermal spectrum of an accretion disk with $T \simeq 5 \cdot 10^4$ K.

Send offprint requests to: H. Lesch

There are at least two pieces of evidence for the presence of relativistic electrons in AGN, first the clear detection of hard X-ray and γ-ray spectra and second the radio observations of superluminous motions on VLBI scales, which describe the existence of a plasma with relativistic bulk motions. Furthermore, the most successful models of X-ray emission in AGN imply the copious production of $e^+ - e^-$ pairs via $\gamma - \gamma$ interactions, preprocessing by inverse Compton scattering of the soft photons emitted by the accretion disk (Svensson 1987; Lightman and Zdiarski 1987; Done and Fabian 1989; Svensson 1990). The main finding of those studies is that for monoenergetic injection of e$^\pm$ at large Lorentz factors ($\gamma \simeq 200$) and for the range $1 < l < 10^2$, the X-ray spectral index is $\alpha \simeq 0.7 \pm 0.15$, which is in general agreement with AGN observations (Svensson 1990). Here l denotes the compactness parameter, given by

$$l \equiv \frac{L\sigma_T}{Rm_e c^3} = \frac{2\pi}{3}\left[\frac{L}{L_{Edd}}\right]\left[\frac{3R_s}{R}\right]. \qquad (1)$$

Here, $L_{Edd} = 2\pi m_p c^3 R_s/\sigma_T$ is the Eddington luminosity, σ_T is the Thomson cross-section, m_e and m_p are the electron and proton masses and $R_s = 2GM/c^2$ is the Schwarzschild radius.

Dermer and Schlickeiser (1993) have shown that the γ-radiation observed from quasars and blazars may originate in a distance R of 10^{2-3} gravitational radii from the central engine. At that distance, the compactness parameter $l < 1$, i.e. no pair production appears. Instead, the relativistic leptons scatter via the inverse Compton process the UV radiation within a relativistically moving jet.

It is the aim of this contribution to consider the problem of rapid charged particle acceleration in the presence of an intense UV radiation field characteristic for the environment of the accretion disk in active galactic nuclei. The UV photons scatter the particles via inverse Compton scattering. The Compton cooling rate of a relativistic electron scattering with a low-energy photon ($h\nu \ll m_e c^2$) is

$$\frac{dE}{dt} \simeq \sigma_T c U_{rad}\gamma^2 \qquad (2)$$

where U_{rad} is the radiation energy density. As U_{rad} can be related to the luminosity L of a source of size R through $U_{rad} \sim$

$L/4\pi R^2 c$ one can write the Compton cooling time scale as

$$t_{cool} = \frac{E}{dE/dt} \sim \left(\frac{R}{c}\right)\frac{10}{\gamma l}. \tag{3}$$

This means that for a compactness $l \simeq 10$ all electrons cool before they can escape ($t_{escape} \geq R/c$). To avoid a pileup of cool particles reacceleration (or annihilation, if the particles come in pairs) is necessary.

The "standard" acceleration mechanisms - diffusive shock wave acceleration and resonant acceleration by magnetohydrodynamical (MHD) turbulence (also known as Fermi I and Fermi II-process) seem to fail since they cannot provide Lorentz factors less than $\gamma_{crit} \simeq \frac{m_p}{m_e}$. This means that particles accelerated via shocks or turbulence have to be preaccelerated - this is also known as the **injection problem** (Blandford 1994; Melrose 1994).

Let us shortly summarize the arguments which lead to the result that particles need γ_{crit} before they can be picked up by the shock wave acceleration process or by resonant acceleration by MHD turbulence:

The threshold γ_{crit} is associated with the requirement of effective damping of the Alfvén waves by the relativistic electrons. The maximum frequency of Alfvén waves is the ion cyclotron frequency $\omega_{ci} = eB/m_i c$. For effective electron acceleration, the relativistic electron gyro frequency $\omega_{ce} = eB/\gamma m_e c$ should be comparable to ω_{ci} (Kuijpers 1996). Therefore we have a minimum Lorentz factor for the electrons in a hydrogen plasma of $\gamma_{min} \simeq m_i/m_e = 1836$.

If acceleration proceeds at a collisionless shock of width Δ, electrons will not see the shock as a discontinuity unless their scattering mean free-path $\lambda_e > \Delta$. Both by observations and numerical simulations (Formisano et al 1975; Winske et al. 1985) one finds that a quasi-parallel collisionless shock has a width of a few times c/ω_{pi}, where $\omega_{pi} = \sqrt{4\pi e^2 n/m_i}$ is the ion plasma frequency. If scattering is due to strong magnetic fluctuations one has $\lambda_e \sim r_g \sim pc/eB$. Electrons will not see the shock as a discontinuity unless $p > eB/\omega_{pi} = m_i v_A$ ($v_A = B/\sqrt{4\pi n m_i}$ is the Alfvén velocity). When the subshock is erased by the diffusive action of accelerated protons, the shockwidth will exceed $\Delta \simeq m_i u_s c/eB$, which is the gyroradius of a proton with momentum $m_i u_s$. Electrons need to have at least the same momentum before shock acceleration becomes efficient. For shock acceleration to operate a shock has to be super-Alfvénic ($u_s > v_A$). Consequently, this requirement proves stronger than the first one.

In all cases some mechanism is needed to preaccelerate electrons to energies exceeding the typical "thermal" energy per particle $m_i u_s^2/2$ in the downstream flow.

It was proposed that Whistler waves with frequencies between the ion and electron-gyrofrequency may solve the injection problem, or at least relax the injection condition down to $\gamma_{min} \simeq \sqrt{m_i/m_e} \sim 43$, since the waves can be in resonance with electrons of this energy (Levinson 1992).

However, there is a significant difference between MHD-turbulence and Whistler turbulence. The MHD-turbulence originates in macroscopic turbulent fluid motions (like winds, jets-etc..). The source scale of the turbulence is much larger then ion gyroradii. The turbulent energy is transferred from large scales via dissipationless cascading down to the small dissipation scale which is approximately the ion gyroradius (e.g. Biskamp 1993). There the particles can be accelerated by the resonant interaction with the MHD-waves. Obviously the large energy reservoir for particle acceleration by MHD turbulence easily explains the high energies in relativistic particles. This is an enormous advantage of the Fermi-processes because in every acceleration model the energy of the accelerator should be larger then the final energy in the accelerated particles.

Such a condition is difficult to achieve for the excitation of Whistler waves since they are driven by phase space anisotropies of the particle distribution function (e.g. Krall and Trivelpiece 1973). To accelerate particles the anisotropy of the distribution has to be enormous in order to excite strong enough Whistler turbulence. The energy density in the waves has to be high enough in order to accelerate particles. Since it is the anisotropy either of distribution function of the background plasma or of a high energy particle beam which is responsible for the excitation of the waves, the required anisotropy means an extreme deviation from a Maxwellian distribution. In other words, the presence of intense Whistler turbulence would mean already a strong preacceleration of electrons in order to get the anisotropic distribution function needed. Because of this requirements we think that Whistler waves are not a real solution of the injection problem.

In this contribution we investigate the possible role of magnetic field-aligned electric fields in the injection problem context. Such fields are related to magnetic field-aligned potential drops, which are known to occur, e.g. in the Earth's magnetosphere at several 1000 km altitudes above auroral arcs. For terrestrial observers auroral acceleration regions are the closest realization of a powerful cosmic acceleration process, relatively easy to probe and indeed documented by a wealth of data (cf. Block and Fälthammar 1990; Lysak 1990). The more one should be surprised that few attempts have been made to transfer the knowledge gained from the Earth's aurora to other cosmical situations. Acceleration in field-aligned electric fields has received much attention in context of pulsar magnetospheres (e.g. Goldreich and Julian 1969; Ruderman and Sutherland 1975) and is thought to occur in solar flares (e.g. Sakai and Ohsawa 1987; Litvinenko 1996). An acceleration process so common to the benign plasma environment of the Earth can be rightly suspected to exist in any cosmic magnetic field that is sufficiently agitated.

Field-aligned potential drops as a product of intense field-aligned electric currents imply the existence of significantly sheared magnetic fields. In the following section we describe how magnetic fields are sheared in the corona of an accretion disk in the vicinity of a black hole. The forces creating the magnetic shear are the ultimate cause of the related acceleration process and supplier of the energy provided for particle acceleration. A prominent feature of this acceleration process is that energy supply and energy conversion (into relativistic electron beams) are physically separated. There is one plasma regime which we identify with the accretion disk, mostly characterized

by a high value of the plasma beta, i.e. the ratio of gas and magnetic pressure ($\beta = 8\pi p/B^2$). The acting of mechanical forces, like friction, pressure gradients, or the inertial force, can not be fully balanced by magnetic forces but require the transport of shear stresses out of the interaction volume into another plasma regime, with low β where the forces are eventually balanced. The transport of shear stresses is effected by field-aligned currents. We will identify the low-β region with the corona of the accretion disk. In Sect. 3 we describe the acceleration region making use of an analytical kinematic model introduced by Schindler et al. (1991). In Sect 4. we introduce a simple dynamical numerical model for the formation of localized regions of significant field-aligned electric fields and describe how electrons are accelerated and under which conditions they can reach large Lorentz-factors in the vicinity of the excessively UV radiating innermost parts of an accretion disk around a massive black hole. A discussion of our findings is given in Sect. 5.

2. Magnetized accretion disks in active galactic nuclei

Active galactic nuclei (AGN) show extremely energetic outflows extending even to scales beyond the outer edge of the galaxy in the form of strongly collimated radio jets (Bridle & Perley 1984; Perley 1989). There is substantial evidence that magnetic forces are involved in the jet driving mechanism (Blandford & Payne 1982; Blandford 1989; Camenzind 1990a,b) and that the magnetic fields will also provide the collimation of the flow, since huge currents are involved in the jet flows (Benford 1978; Heyvarts & Norman 1989; Lesch et al., 1989).

A Keplerian accretion disk has been found beyond any doubt in the mildly active galaxy NGC 4258 (Miyoshi et al. 1995). Additionally, at least in some cases the AGN show some evidence for rotating accretion disks. These objects exhibit the classical double-peaked, broad emission lines which are considered to be characteristic for a Keplerian rotating disk. Standard thin disks do, however, not release sufficient gravitational energy locally at the radii, where the Keplerian velocity corresponds to the observed width of the emission lines (typically at $\simeq 10^3$ Schwarzschild radii). Some extra source of energy is required (Collin-Souffrin 1987), which could be found in the interaction of an accretion disk with the corona of the AGN.

Therefore, we consider as a possible scenario a rotating black hole surrounded by a magnetized accretion disk (Camenzind 1990a,b). The origin of the magnetic fields in accretion disks must be due to the existence of seed fields in the disks which extend to larger scales of a few parsecs to a few hundreds of parsecs in galaxies (Begelman et al. 1989). These larger disks and rings represent reservoirs for gas and magnetic flux which are accreted onto the central black hole.

As the plasma of the disk is accreted in the gravitational potential of the central object, magnetic field lines are convected inwards, amplified and finally deposited at the horizon of the black hole. A dynamo in the disk may be responsible for the maintenance and amplification of the magnetic field in the disk (for the details of dynamo action in accretion disks, see Khanna
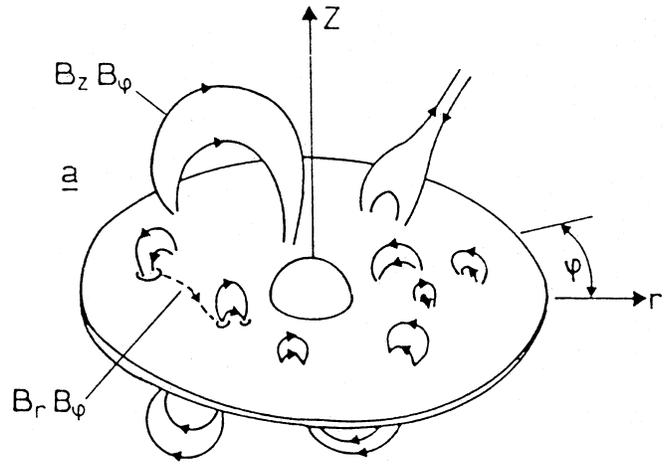

Fig. 1. Hydromagnetic phenomena in thin accretion disks and the buildup of a corona. Whenever the magnetic field in the disk (generated by a dynamo) is in equipartition with the amplifying forces (differential shear and convective motions), magnetic flux tubes, convective turbulent cells, etc. will ascend and feed magnetic energy into the corona. If the driving forces cannot be counteracted by normal magnetic stresses in the disk, the field lines are bent in the direction of the force and currents parallel to the magnetic field propagate into the corona. To close the current circuit it is necessary to drive perpendicular currents somewhere in the corona. Moreover, in order for a current to flow, a resistor (load) within the circuit is necessary (Ohm's law). This leads to localized dissipative regions, where magnetic energy is transferred into particle energy via field-aligned electric fields.

and Camenzind (1994). The interplay of differential rotation and convective turbulence (ascending (descending) turbulent cells) amplifies the magnetic field whereas processes like magnetic buoyancy limit further amplification (Stella & Rosner 1984). An inevitable consequence of convective turbulence and magnetic buoyancy is the formation of a hot, magnetically active corona due to the transfer of magnetic energy to the coronal plasma (see Fig. 1).

The significance of coronal dissipation is clearly indicated by X-rays and γ-rays observations of quasars (Maraschi et al. 1989; Dermer and Schlickeiser 1993) which show that the emission cannot originate in a thin disk since the disk temperatures do not exceed 10^5 K (Straumann 1986), but must be emitted in the corona and jet, respectively. The UV disk photons are Compton scattered by the hot or relativistic coronal electrons and positrons. Zdiarski et al. (1993) argue that the observations of the Seyfert galaxy NGC 4151 in hard X-rays and in γ-rays are well explained by a nonthermal model with acceleration of relativistic electrons at an effiency of $\leq 50\%$. The particles loose energy via inverse Compton scattering of UV photons and are continuously reaccelerated to Lorentz factors of a few hundred. We note again that such an acceleration is not possible via Fermi-processes, because the necessary energies of the particles are below $\gamma_{crit} \simeq 1836$. We emphasize that the observed flux variations in the optical and UV ranges are too fast to be caused by the variations of the accretion rate only.

It was proposed (Ulrich 1991) that instabilities at the inner part of the disk are a possible origin for these fast variations. Evidences for localized dissipation regions are also given by global models for the origin of relativistic jets in AGN (Camenzind 1990a). Such models contain a rotating, supermassive black hole, surrounded by a magnetized accretion disk and a corona. The relativistic jet velocities are caused by magnetic acceleration and the collimation of the outflows is produced by currents flowing along the jet axis. If the electric current is resolved into a field-aligned current $\mathbf{J}_{\parallel}$ and a current perpendicular to the magnetic field $\mathbf{J}_{\perp}$, one can relate $\mathbf{J}_{\parallel}$ to $\mathbf{J}_{\perp}$ by $\nabla \cdot \mathbf{J}_{\parallel} = -\nabla \cdot \mathbf{J}_{\perp}$ on the grounds of current conservation. In the considered scenario the plasma in the corona is coupled electrodynamically with the plasma in the accretion disk by field-aligned electric currents. $\mathbf{J}_{\parallel}$ therefore represents the means by which the magnetic energy is transported from the generator (the disk with $-\nabla \cdot \mathbf{J}_{\perp}$) to its "storage" site. The generation of perpendicular currents in the accretion disk is the result from mechanical forces of the differential shear acting on the disk magnetic field. Whenever the magnetic field in the disk (generated by a dynamo) is in equipartition with the amplifying forces (differential shear and turbulent motions) magnetic flux tubes, convective turbulent cells, etc. will ascend, which by driving field-aligned currents feed magnetic energy into the corona. In other words, if the driving forces cannot be balanced by normal magnetic stresses in the disk the field lines are bent in the direction of the force and currents parallel to the magnetic field propagate into the corona (see Fig. 1). The closure of the current circuit will be provided alternatively by flux tubes bending back to the disk surface or by perpendicular currents in the corona.

Summarizing, if a differentially rotating accretion disk accretes magnetized gas, the formation of an electrodynamically coupled corona is unavoidable. The transfer of shear stresses is effected via field-aligned currents. A concentration of electric energy in thin sheets increases the current density. The formation of field-aligned potential drops depends sensitively on the actual value of the current density.

3. A kinematic description of field-aligned electric potential drops in the corona of an accretion disk

Magnetic fields have long been considered as an important element in the dynamics of accretion disks, primarily as a mechanism for supplying internal stresses required for efficient angular momentum transfer (Eardley and Lightman 1975; Ichimaru 1977; Hawley and Balbus 1991, 1992). In these models magnetic fields can be generated within the inner portion of an accretion disk by the joint action of thermal convection and differential rotation along Keplerian orbits. Field amplification will then be limited by nonlinear effects; as a consequence of buoyancy, magnetic flux will be expelled from the disk, leading to an accretion disk corona consisting of many magnetic loops where the energy is stored and probably transferred via magnetic reconnection into heat and particle acceleration.

The buildup of magnetic fields within the disk is limited by nonlinear effects related to convection. Since convection takes place primarily perpendicular to the plane of the disk, we shall assume differential rotation to remain the dominant mechanism for the toroidal magnetic field B_T generation; the generation of the poloidal field B_P will then be dominated by convection-mediated effects. For convection cells whose aspect ratio is $\sim O(1)$, the poloidal magnetic field spatial scale will then be of the order of the convective cell size H, equal to the half-thickness of the disk. To describe the generation of B_P we invoke magnetic flux conservation:

$$B_P \simeq \frac{H}{R} B_T. \tag{4}$$

The maximal toroidal field strength is given by the energy density of the turbulence in the disk (Galeev et al. 1979)

$$\frac{B_T^2}{8\pi} \simeq n_e m_i c_s^2, \tag{5}$$

where $c_s = \sqrt{\frac{k_B T}{m_i}}$ denotes the sound velocity.

The temperature $T(R)$ of the disk is given by (Straumann 1986)

$$T(R) \simeq T_{in} \left[\frac{R_{in}}{R} \right]^{0.75}, \tag{6}$$

with the temperature at the inner edge $R_{in} \simeq 3R_S$ of the disk

$$T_{in} = 10^5 \, \text{K} \left[\frac{M_{BH}}{10^8 \, \text{M}_\odot} \right]^{-1/4} \left[\frac{\dot{M}}{1 \, \text{M}_\odot \text{yr}^{-1}} \right]^{1/4}. \tag{7}$$

Here we use the accretion rate $\dot{M}$. This temperature corresponds to a sound velocity of $3 \cdot 10^6 \, \text{cms}^{-1}$

With the same parameters for the particle density we obtain a central value of about $n \simeq 4 \cdot 10^{14} \, cm^{-3} (R/R_{in})^{-3/2}$. We get the maximum toroidal field strength of about $B_T \simeq 500 \, \text{G}$ or a poloidal field of about $B_P \simeq 50 \text{G}$, respectively.

Field-aligned electric fields can be discussed either in terms of generalized Ohm's law

$$c\mathbf{E} = -\mathbf{v} \times \mathbf{B} + \mathbf{R} \tag{8}$$

where $\mathbf{E}$, $\mathbf{v}$ and $\mathbf{R}$ denote the electric field, the plasma velocity and some unspecified nonidealness $\mathbf{R}$. One either has to specify for the parallel component of the nonidealness $\mathbf{R}$ or one can explore definite properties of the magnetic field and the plasma flow that necessarily imply a significant field-aligned electric field on the grounds of a kinematic approach (Schindler 1991; Schindler et. al 1991). The formation of such parallel electric fields can be understood as a consequence of some driving voltage $\int |\mathbf{v} \times \mathbf{B} d\mathbf{s}|$ (where the integration is carried out along a magnetic line element $d\mathbf{s}$) and a local violation of ideal Ohm's law (cf. Schindler et al., 1991; Kuijpers, 1996).

It is a matter of question which processes lead to current concentrations and thereby to $\mathbf{R} \neq 0$. Possible mechanisms are superheating-instabilities (Coppi and Friedland 1971; Coppi 1975; Spicer 1976) radiation induced instabilities (Schmutzler and Lesch 1989) or various kinds of current-driven microinstabilities (Lesch 1991), in particular the lower-hybrid-drift and the

ion-cyclotron drift instabilities that are distinguished from others by their rather non-stringent onset criteria (cf. Papadopoulos 1979; Huba 1985).

Obviously, the kinematic approach in terms of magnetic field and the flow patterns bypasses the physical foundation of a specified violation of ideal Ohm's law, e.g. the microscopic mechanism by which field-aligned currents become unstable and give rise to localized regions of anomaleous momentum transfer. Making use of this approach one has to discuss the relevant quantity (cf. Hesse and Schindler 1988)

$$U = - \int E_{||} ds \qquad (9)$$

where the integral is extended over the arc length of a given magnetic field line ds. The quantity U is to be understood as a "generalized" field-aligned electric potential that for a steady state configuration is identical to the electrostatic potential. Schindler et al. (1991) show that U has to satisfy the following equations

$$\left[\frac{d\beta}{dt}\right] = \frac{\partial U}{\partial \alpha} c \qquad (10)$$

and

$$\left[\frac{d\alpha}{dt}\right] = -\frac{\partial U}{\partial \beta} c \qquad (11)$$

Here, α and β denote the Euler potentials ($\mathbf{B} = \nabla\alpha \times \nabla\beta$) and the brackets denote differences in the quantities on either sides of the nonidealness along magnetic field lines. Thus, Eqs. (10) and (11) show that the difference in the magnetic field and the plasma flow on either side outside the nonideal region is a measure for the generalized potential U. This measure does not depend explicitly on the rather involved physics that support the anomaleous dissipation required for $E_{||} \neq 0$.

We define appropriate Euler potentials by assuming an almost bipolar magnetic field, which implies $\alpha \sim m_c sin^2\vartheta/R_c$ where ϑ is the azimuthal angle in spherical coordinates and m_c and R_c denote the dipole moment and the radius of the central compact object. If one maps the values for α and the poloidal angle Φ into the corona of the AGN by keeping them constant, Euler potentials are defined as $\mathbf{B} = \nabla\alpha \times \nabla\Phi$. From Eq. (10) we get an order of magnitude estimation for U:

$$U \approx \frac{\Delta\alpha\Delta\Phi}{c\Delta t} \qquad (12)$$

The typical magnetic flux in Quasar jets is found to be $\approx 10^{34}$Gcm^{-2} (Standke et al. 1996). In order to accelerate electrons up to $\gamma \simeq 1800$ we need a generalized potential drop $U \simeq 3 \cdot 10^6$statvolt. Thus, if we think about intraday variability (cf. Standke et al.1996), which gives an upper limit of $\Delta t \sim 8.6 \cdot 10^4$s, and assume a latitudinal width of the acceleration region of the order of $\Delta\Phi \approx 20°$ the poloidal magnetic flux difference has to be $\Delta\alpha \approx 6 \cdot 10^{20}$Gcm^{-2}, i.e. only a small amount of the total magnetic flux is associated with the acceleration process. If we assume the acceleration region to be located in a distance of about $50R_S$ ($R_S = 2GM_{BH}/c^2$ is the Schwarzschild radius of the central object), which implies

$B \approx 2 \cdot 10^3$G for a magnetic field profile $B_{pol} = 10^5 R^{-1}$G and $B_{tor} = 0.1 B_{pol}$, the region of $U \neq 0$ covers an area of about $3 \cdot 10^{17}$ cm^2. For any effective particle acceleration the length of the acceleration region λ_{acc} must not exceed the loss length due to synchrotron radiation

$$\lambda_{losssyn} \approx \frac{5 \cdot 10^8 c}{B_{pol}(R)^2 \gamma_{crit}}. \qquad (13)$$

In the considered physical situation this implies current sheets with widths of the order of $\omega \approx 1.5 \cdot 10^{10}$ cm with $\lambda_{acc} \approx \lambda_{losssyn}(\gamma = 1800, R = 50R_S) \approx 10^9$ cm (cf. Sect. 5). However, we note that variability on shorter time scales allows for thinner current sheets.

4. A dynamical numerical model for the formation of field-aligned potential drops in the corona of an accretion disk

In this section we study the formation of localized field-aligned electric fields in the corona of an AGN in a idealized dynamical numerical model. For this we use a Cartesian (for simplicity we choose a slab geometry) 3D resistive MHD code that integrates the following balance equations:

$$\frac{\partial \rho}{\partial t} + \nabla \cdot (\rho\mathbf{v}) = 0 \qquad (14)$$

$$\frac{\partial}{\partial t}(\rho\mathbf{v}) + \nabla \cdot (\rho\mathbf{vv}) = -\nabla p + \mathbf{j} \times \mathbf{B} \qquad (15)$$

$$\frac{\partial p}{\partial t} + \nabla \cdot (p\mathbf{v}) = \frac{2}{3}(-p\nabla \cdot \mathbf{v} + \eta j^2) \qquad (16)$$

$$\frac{\partial \mathbf{B}}{\partial t} = \nabla \times (\mathbf{v} \times \mathbf{B}) + \nabla \times (\eta\mathbf{j}) \qquad (17)$$

Here, ρ, $\mathbf{v}$, p and η denote the plasma density, velocity and pressure and the (anomaleous) resistivity. The code makes use of an explicit difference scheme based on the Leapfrog algorithm that is second order in space and time (cf. Otto 1993). The principle train of thought is the following (cf. Otto and Birk 1993; Birk and Otto 1996): The different convective plasma motion at different regions of the coronae of AGN or differential shear motion of the disk itself results in a magnetic shear and thereby the origin of field-aligned electric currents. When this convective shear motion is strong enough the current density exceeds some critical value and current-driven microinstabilities are excited which in course of their nonlinear saturation lead to an anomaleous resistivity. The excitation of microinstabilities can be regarded as a special case of $\mathbf{R} \neq 0$ in Ohm's law as discussed in the previous section. We note that the necessary onset condition for the scenario we have in mind is any violation of ideal Ohm's law that allows for $\mathbf{E}_{||} \neq 0$; we just concentrate on $\eta\mathbf{j}$- nonidealities for illustration purposes. The formation of localized regions of anomaleous dissipation gives rise to the onset of magnetic reconnection. During the nonlinear dynamical evolution very localized acceleration regions with fairly high field-aligned electric fields form. In these potential structures electrons can in principle be accelerated up to energies of

$\gamma \simeq 1800$. In this section we show results for an exemplary chosen set of parameters. Parts of a realistic parameter space and, in particular, consequences of different altitudes and extensions of the acceleration region for the physical situation under consideration are discussed in the following section.

We consider one single sheared coronal loop (see Fig. 1), i.e. a magnetic flux tube with a current flowing due to the magnetic shear. Since we are mainly interested in the region $\mathbf{R} \neq 0$ we do not have to take into account coronal current closure. An appropriate idealized initial configuration for the numerical simulation is the following force-free magnetic field, given by (cf. Birk and Otto 1996):

$$\mathbf{B} = B_{y0} \tanh(x)\, \mathbf{e}_y \; - \sqrt{B_{z0}^2 + \frac{B_{y0}^2}{\cosh^2(x)}}\; \mathbf{e}_z \qquad (18)$$

where B_{z0} and B_{y0} denote the constant main component and the shear (toroidal) component of the magnetic field, respectively. The choice provides us with a generic magnetic field configuration with a current sheet due to magnetic shear. An alternative choice would be $\mathbf{B} = B_{y0} tanh(x)$ which would require some pressure profile $p \sim cosh^{-2}(x)$ whereas in the present approach we could start with a homogeneous plasma. We note that the actual choice does not alter the results significantly as long as we deal with a current sheet with $\mathbf{j} \cdot \mathbf{B} \neq 0$.

We note that we study a single thin acceleration region, as a part of an extended relatively thin current sheet, at about $R \approx 50 R_S$. It is to expected that a number of such regions at different altitudes and latitudes permanently form due to the mechanical shear forces (cf. Sect. 2).

The change of B_{y0} through the current sheet ΔB_{y0}, the half-width of the latter ω and the critical current density j_{crit}, are related by Ampère's law:

$$\omega = \frac{c|\Delta B_{y0}|}{8\pi j_{crit}}. \qquad (19)$$

The threshold current j_{crit} for microinstabilities can be related to the critical drift velocity $\mathbf{v}_{crit}$ (cf. Papadopoulos 1979) by $j_{crit} = e n_e v_{crit}$. Since the currents are generated by shearing forces in the disk with $\beta \simeq 1$ and transmitted along the magnetic field lines into the corona with $\beta < 1$, we expect the critical drift speed $v_{crit} \approx f v_i$ (v_i is the ion thermal velocity). The value of the scaling factor, f, depends on the prevailing kind of microinstability, which in turn, depends on the local plasma parameters (cf. Papadopoulos 1979; Huba 1985). For our order of magnitude estimations we choose f of the order of unity. Notwithstanding the uncertainty of the current concentration process in most cosmical applications we obtain for the half-width of the current generated by the mechanical shear forces $\omega \approx 10^7$ cm, if we assume a shear magnetic field of $B_{y0} = 200$G and a critical current density of $j_{crit} = e n v_i \approx 10^4$statampcm^{-2} ($v_i$ is the ion thermal velocity) with $n = 3 \cdot 10^5$ cm^{-3} (as a density profile we assume $n(R) = 10^8 R^{-1.5}$ cm^{-3}) and $T_i = 10^8$K (cf. Ulrich 1991; Nandra and Pounds 1994), With these values the electric field is normalized to $E_0 = v_A B_{y0}/c \approx 200$statvoltcm^{-1} ($v_A$ is the shear Alfvén velocity $v_A = B_{y0}/\sqrt{4\pi n_0 m_i} = c$).
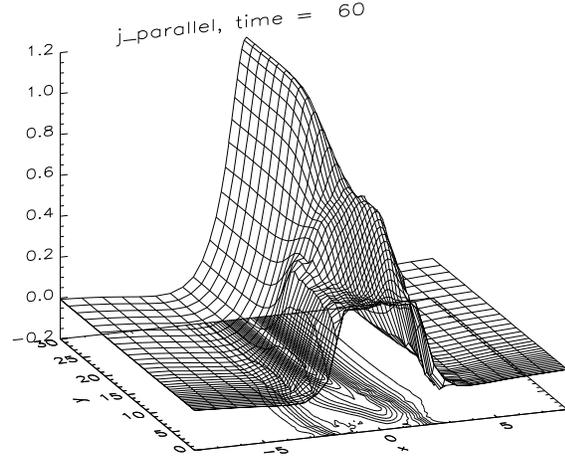

Fig. 2. Surface plot of the field-aligned current density at $z = 40$ after $t = 60\tau_A$. The reduction of the current density (up to 20% of the initial value chosen as 1 in normalized units) caused by the resistive instability is evident.

The magnetic Reynoldsnumber depends on the actual kind of microinstability that is excited. If we assume the excitation of the ion-cyclotron-drift turbulence the resulting anomaleous resistivity is $\eta_{ic} = m_e/ne^2\Omega_i \approx 3 \cdot 10^{-7}$s maximum (cf. Papadopoulos 1979; Huba, 1985), where Ω_i is the ion-cyclotron frequency, and thus, the magnetic Reynoldsnumber reads $S = 4\pi v_A\omega/\eta_{ic}c^2 \approx 6 \cdot 10^4$. We note that the lower-hybrid-drift instability would result in a slightly lower resistivity. For numerical reason we use a somewhat lower magnetic Reynoldsnumber $S = 10^3$ and rescale our quantitative findings accordingly.

In order to model a macroscopic resistive instability at an altitude H in the corona of an AGN (caused by supercritical currents) we apply the following velocity perturbation as an initial condition:

$$v_y(x, z, t) = v_{y0} \frac{\tanh(2x)}{\cosh^2\left(\frac{x}{3}\right)} \exp\left(-\frac{z}{6}\right). \qquad (20)$$

As a boundary condition for $t > 0$ we use

$$v_y(x, z_{min}, t) = v_{y0} \frac{\tanh(2x)}{\cosh^2\left(\frac{x}{3}\right)}. \qquad (21)$$

These velocity perturbations with an amplitude chosen as $v_{y0} = 0.5\%$ of the Alfvén velocity mimic differential or convective plasma motion at one end of the considered coronal loop that due to the quasi-ideality of the plasma leads to a further shear of the magnetic field and an increase of the field-aligned current density. An anomaleous resistivity will be switched on if this current density exceeds a critical value j_{crit} (we start with a marginal current density), and thus, gives rise to the macroscopic resistive instability. We localize the resistivity in the z-direction in order to model an acceleration region of the length of 15ω extended along the poloidal magnetic field.

For the numerical realization we pose line symmetry as boundary conditions in the y-direction and carry out the simulations with 49 grid points in x-direction, 39 grid points in
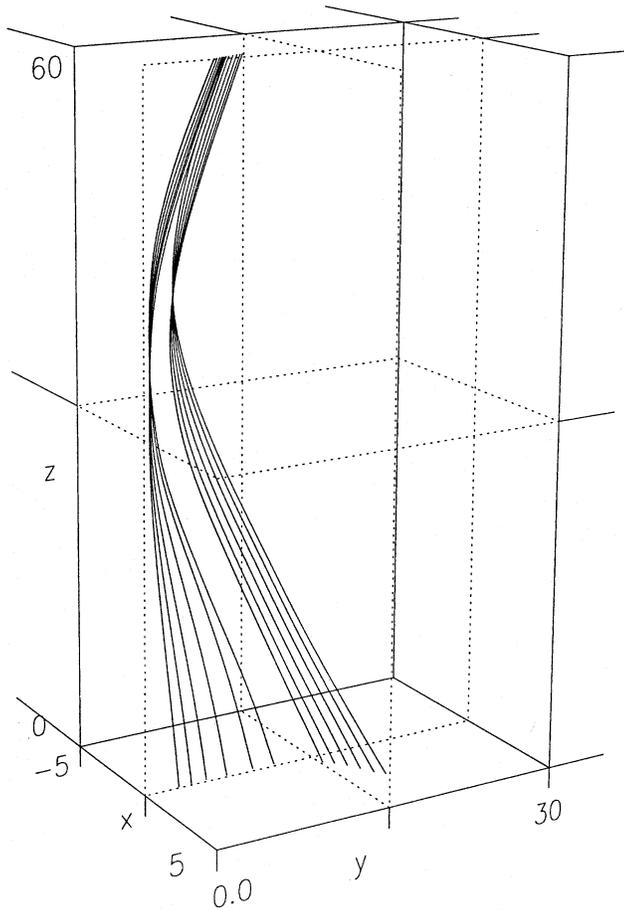
Fig. 3. Perspective view of magnetic field lines having a very central (field lines on the left hand side) or more remote trajectory through the acceleration region

Fig. 4. Surface plot of the magnetic field-aligned component of the electric field at $z = 40$ after $t = 120\tau_A$. The field-aligned electric field may result in coherent acceleration of charged particles.

y-direction, and 105 grid points in z-direction, where we use a non-uniform numerical grid with a maximum resolution of 0.05 in the x- and z-direction, 0.4 in the y-direction, and 0.2 in the z-direction. The dimensions of our numerical box are given by $x \in [-10, 10]$, $y \in [0, 30]$, and $z \in [0, 60]$ in normalized units with a scaling length of $\omega = 4 \cdot 10^7$ cm, the half-width of the field-aligned current layer. Once again it should be noted that we mainly model the dissipative part of the (in the z-direction, i.e. parallel to the main component of the magnetic field) extended current sheet which at significant higher and lower altitudes is assumed to be ideal.

During the dynamical evolution of the resistive instability the field-aligned current density is reduced as shown in the snapshot after 60 Alfvénic transit times $\tau_A = \omega/v_A$ (Fig. 2) (the initial current density was chosen as 1 in normalized units). This reduction appears due to the fact that magnetic energy stored due to the shear can now be released and is converted in bulk kinetic energy as well as thermal energy during the instability process.

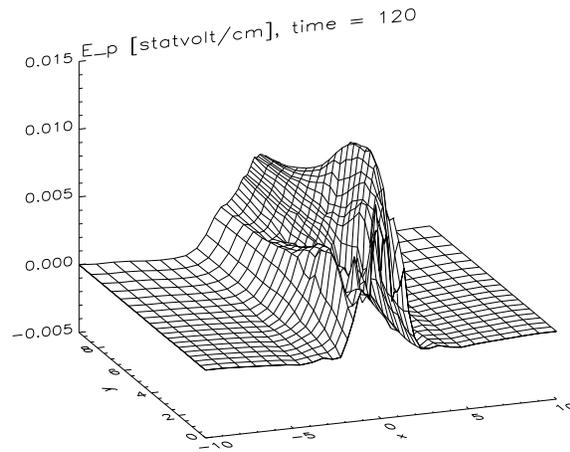Fig. 3 shows a perspective view of magnetic field lines. One set of field lines traverse the entire acceleration region whereas the other one represents flux that has been reconnected slightly earlier.

The main point is that during the dynamics a relatively strong field-aligned electric field ($E_{||} = \eta(j_{||})j_{||}$) evolves very fast $120\tau_A \sim 0.1$s ($v_A \simeq c$, $\omega \sim 3 \cdot 10^7$ cm) that grows up to a maximum value of $E_p^{max} = 0.012$ statvoltcm^{-1} for the parameters chosen (Fig. 4).

Since the strength of the electric field depends in particular on the magnitude of the resistivity (or the magnetic Reynolds-number) and the critical current density, our quantitative results are to be understood as rough but quite realistic order of magnitude estimations. The evolving field-aligned electric fields can accelerate charged particles as it is the case in so-called "auroral potential structures" observed in the Earth's magnetosphere (cf. Mozer 1981) and consequently may play an important role for the solution of the injection problem.

Fig. 5 shows the generalized electric potential U (obtained by integrating the field-aligned electric field along magnetic field lines that penetrate the $\mathbf{R} \neq 0$-region) evolving during the nonlinear instability dynamics. Similar to the Earth's auroral acceleration regions thin elongated regions "potential" structures form. Assuming a central acceleration region localized at $50R_S$ (again we note that for $\eta\mathbf{j}$-nonidealities the actual location of the acceleration region depends on the local plasma parameters allowing for localized dissipation) electrons can in principle be accelerated along the poloidal magnetic field up to a Lorentz factor of $\gamma \simeq eU/m_e c^2 = 1800$. However, this quantitative result obtained by the simulations is to be understood as an upper limit. In order to arrive at a fully consistent description particle simulations has to be performed with the input parameters for the electric and magnetic field given by the MHD simulations. The resulting particle distribution function has to be analyzed carefully in order to evaluate the effectiveness of the reconnection process in some detail. This task is beyond the scope of this contribution, in which we are restricted to a more qualitative level showing that reconnection is important from order of
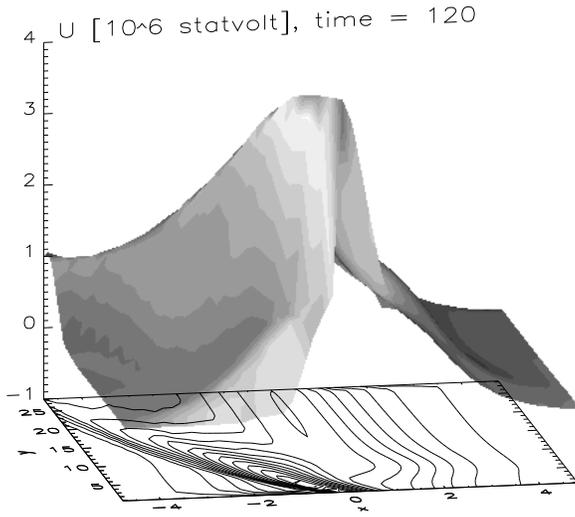
Fig. 5. The generalized electric potential U after $t = 120\tau_A$. Similar to the Earth's auroral acceleration regions a thin elongated structure evolves with a maximum of $U_{max} = 3.8 \cdot 10^6$ statvolt. In such regions charged particles can in principle be accelerated up to $\gamma \simeq 1800$.

magnitude estimations, and will be dedicated to future investigations.

5. Summary and discussion

In this contribution we introduced the idea that magnetic field-aligned electric fields may contribute significantly to the high number density of relativistic particles required in the AGN context. We proposed that macroscopic resistive instability processes or more generally magnetic reconnection may result in the preacceleration of leptons up to $\gamma \approx 1800$. Our approach was twofold: On the one hand, we made use of a kinematic description introduced by Schindler et al. (1991) without specifying for any microscopic dissipation mechanism. We showed that in the framework of kinematic reconnection the formation of acceleration regions with reasonable dimensions length scales ($\lambda_{acc}^{kin} \approx 10^9$ cm and $\omega \approx 10^{10}$ cm) can be described even for relatively long time scales involved in the activity process (intraday variability). On the other hand, we performed numerical simulations in order to study the dynamics in more detail for concrete physical specifications. We showed that for relatively strong magnetic fields leptons can be accelerated along the main component of the magnetic field up to the required energies on a length scale of $\lambda_{acc} = 4 \cdot 10^8$ cm, if we assume the ion-cyclotron microturbulence as a plausible candidate for anomaleous dissipation which implies the existence of current sheets of the width of $\omega \sim 10^7$ cm. However, it is a necessary condition for the acceleration mechanism to operate effectively that the acceleration length is shorter than the loss lengths due to either synchrotron radiation or inverse Compton scattering $L_{lossic} = 3 \cdot 10^6 c/U_{rad}\gamma_{crit}$ (which one of the loss process is more important mainly depends on the actual strength of the magnetic field). The relevant length scales for the physical parameters $B_{pol} = 10^5 R^{-1}$G, $B_{tor} = 0.1 B_{pol}$ (i.e
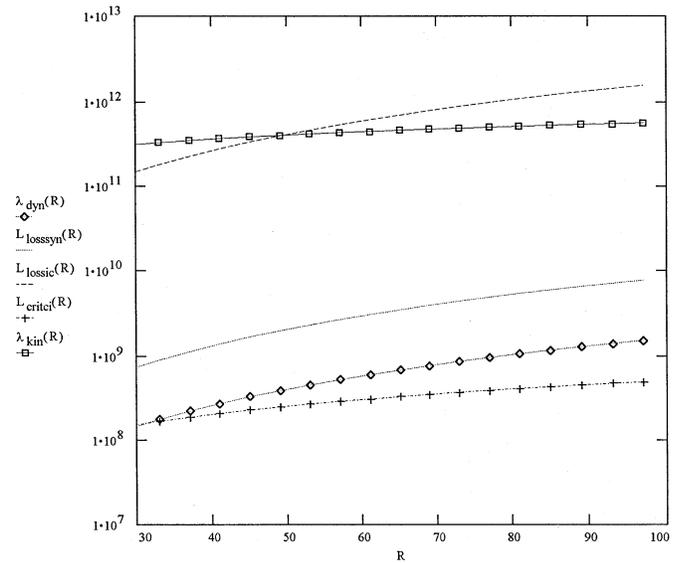

Fig. 6. The relevant loss and acceleration length scales as functions of the distance of the central acceleration region to the central object for $B_{pol} = 10^5 R^{-1}$. In this plot λ_{acc}^{dyn}, λ_{acc}^{kin}, L_{critci}, $L_{losssyn}$ and L_{lossic} denote the acceleration lengths according to the numerical dynamical simulations and the kinematic approach, the critical acceleration length $\lambda_{1836} = 1836 m_e c^2/eE_p^{max}$ and the loss lengths due to synchrotron radiation and inverse Compton scattering, respectively.

$B_{tor}(R = 50R_S) = 200$G, $E(R = 50R_S) = 200$statvoltcm^{-1}), $\omega(R = 50R_S) = 4 \cdot 10^7$cm, $S(R = 50R_S) = 6 \cdot 10^4$, $T = const = 10^8$K, $n = 10^8 R^{-1.5}$ cm^{-3} and $\gamma = 1836$ are illustrated in Fig. 6. It shows the loss lengths due to synchrotron radiation as well as inverse Compton scattering, the acceleration lengths both according to the numerical simulations and the kinematic approach and the critical acceleration length $\lambda_{1836} = 1836 m_e c^2/eE_p^{max}$ which is defined by assuming that the field-aligned electric field (E_p) has the maximum strength obtained by the simulations E_p^{max} under the assumption of ion-cyclotron microturbulence all along the acceleration region. One recognizes that for the chosen magnetic field strengths synchrotron losses dominate losses due to inverse Compton scattering. Both the critical and the dynamical acceleration length are well below the synchrotron loss length, i.e. the particles can be accelerated up to the maximum energies supported by the potential structures. Within the kinematic description the width of the current sheet has to be enlarged by two orders of magnitude in order to receive effective acceleration as long as one deals with the entire time scale of intraday variability.

We note that the synchrotron loss length is overestimated, since it is assumed that the particles are isotropic in pitch angle Ψ. The isotropization time is proportional to the inverse of the ion gyrofrequency, which is much larger then the acceleration time of about $\omega/c \sim 10^{-3}s$. Thus, we cannot expect to have an isotropic energy distribution. For anisotropic distributions it was shown by Epstein (1973) that the loss length is larger then the isotropic loss length by a factor $\Psi^{-2} \propto \gamma^2$. In the case of an anisotropic distribution the length scale for synchrotron
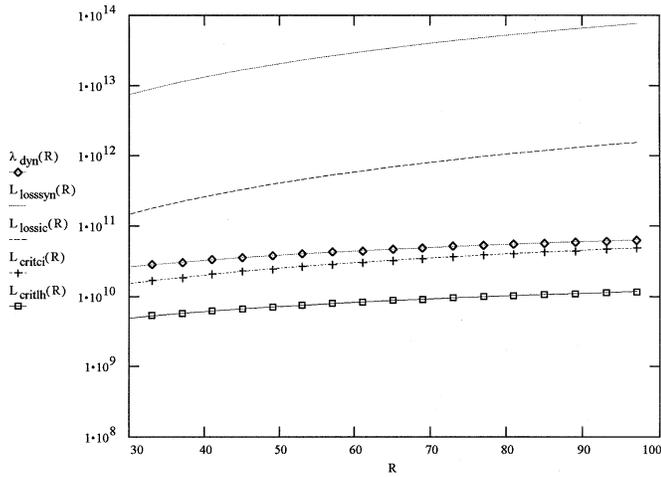
Fig. 7. The relevant loss and acceleration length scales as functions of the distance of the central acceleration region to the central object for $B_{pol} = 10^3 R^{-1}$. In this plot λ_{acc}^{dyn}, L_{critci}, L_{critLH}, $L_{losssyn}$ and L_{lossic} denote the acceleration length according to the numerical simulations, the critical acceleration length $\lambda_{1836} = 1836 m_e c^2 / e E_p^{max}$ assuming ion-cyclotron λ_{critic} or lower-hybrid-drift turbulence λ_{critLH} and the loss lengths due to synchrotron radiation and inverse Compton scattering, respectively.

radiation is 10^6 times larger then the synchrotron loss length for an isotropic distribution.

How does the situation change if the magnetic field is considerably weaker? Fig. 7 shows the relevant length scales for $B_{pol} = 10^3 R^{-1}$ which implies $B_{tor}(R = 50R_S) = 2G$, $E(R = 50R_S) = 0.056 \text{statvoltcm}^{-1})$, $\omega(R = 50R_S) = 4 \cdot 10^5$ cm and a magnetic Reynoldsnumbers of $S(R = 50R_S) = 9 \cdot 10^2$ for the case of lower-hybrid-drift turbulence and $S(R = 50R_S) = 5 \cdot 10^3$ for the case of ion-cyclotron turbulence. Obviously, in this case inverse Compton scattering is the dominant loss process and dissipation caused by the lower-hybrid-drift turbulence results in a shorter acceleration length than dissipation caused by the ion-cyclotron turbulence. What is more, the critical acceleration lengths as well as the dynamical one for the ion-cyclotron instability (the one for the lower-hybrid-drift instability is even shorter) are shorter than the relevant loss lengths.

We conclude that for a fairly large parameter regime in the AGN context resistive instabilities that can be regarded as generic magnetic reconnection processes may play an important role in the preacceleration of charge particles up to energies of 1 GeV, i.e. $\gamma \approx 1800$. The central result of our calculations is that field-aligned potential drops driven by sheared magnetic fields can act as extremely fast accelerators for leptons even in the presence of strong magnetic fields and/or intense radiation field. Future work on relativistic particle simulations for the obtained macroscopic electric and magnetic field configurations is under way in order to corroborate our model.

References

Begelmann, M.C., Shloshman, K.G., Frank, J.: 1989, in Theory of Accretion Disks, eds. F. Meyer, W.J. Duschl, J. Frank and E. Meyer-Hofmeister, Kluwer, Dordrecht, p. 225

Benford, G.: 1978, MNRAS 183, 29

Birk, G.T., Otto, A.: 1996, J. Atm. Sol.-Terr. Phys., in press

Biskamp, D., 1993 Nonlinear Magnetohydrodynamics, Cambridge University Press

Blandford, R.D., Payne, D.G.: 1982, MNRAS 199, 883

Blandford, R.D.: 1989, in Theory of Accretion Disks, eds. F. Meyer, W.J. Duschl, J. Frank and E. Meyer-Hofmeister, Kluwer, Dordrecht, p. 35

Blandford, R.D.: 1994, ApJS 90, 515

Block, L.P., Fälthammar, C.-G.: 1990, J. Geophys. Res. 95, 5877

Bridle, A.H., Perley, R.: 1984, ARAA 22, 319

Camenzind, M.: 1990a, in Galactic and Intergalactic Magnetic Fields IAU 140, eds. R. Beck, P.P. Kronberg, R. Wielebinski, Reidel (Dordrecht), 413

Camenzind, M.: 1990b, in Reviews in Modern Astronomy 3

Collin-Souffrin, S.: 1987, A&A 179, 60

Coppi, B., Friedland, A.B.: 1971 ApJ 169, 379

Coppi, B: 1975, ApJ 195, 545

Dermer, C.D., Schlickeiser, R.: 1993, ApJ 416, 458

Done, C., Fabian, A.C.: 1989, MNRAS 240, 81

Epstein, R.I.: 1973, ApJ, 183, 591

Formisano, V., Russell, C.T., Means, J.D. et al.: 1975, JGR 80, 2013

Galeev, A.A., Rosner, R., Vaiana, G.: 1979, ApJ 229, 318

Goldreich, P., Julian, W.H.: 1969, ApJ 157, 869

Hawley, J.F., Balbus, S.A.: 1991, ApJ 376,223

Hawley, J.F., Balbus, S.A.: 1992, ApJ 400,595

Hesse, M., Schindler, K.: 1988, JGR 93, 5559

Heyvaerts, J., Norman, C.A.: 1989, ApJ 347, 1055

Huba, J.D.: 1985, in Unstable Current Systems and Plasma Instabilities in Astrophysics, IAU107, eds. M.R. Kundu, G.D. Holman, Reidel, Dordrecht, p. 315

Khanna, R., Camenzind, M.: 1994, ApJ 435 L129

Krall, N.A., Trivelpiece, A.W.: 1973, Principles of Plasma Physics, Wiley, New York

Kuijpers, J.: 1996, in Plasma Astrophysics, eds. C. Chiuderi and G. Einaudi, Springer, Heidelberg, p. 101

Lesch, H., Appl, S., Camenzind, M.: 1989, A&A 225, 341

Lesch, H.: 1991, A&A 245, 48

Levinson, A.: 1992, ApJ 401, 73

Lightman, A.P., Zdiarski, A.A.: 1987, ApJ 319, 643

Litvinenko, Y.E.: 1996, ApJ 462, 997

Lysak, R.: 1990, Space Sci. Rev. 52, 1514

Maraschi, L., Maccaraco, T., Ulrich, M.H.: 1989, BL Lac Objects, Lecture Notes in Physics, Springer, Berlin

Melrose, D.B.: 1994, in Plasma Astrophysics, eds. A.O. Benz and T.J.-L. Courvoisier, Springer, Heidelberg, p. 113

Miyoshi, M., Moran, J., Herrnstein, J. et al.: 1995, Nat. 373 127

Mozer, F.S.: 1981, in Physics of Auroral Arc Formation, edited by S.-I. Akasofu and J.R. Kan, pp. 136-142, AGU, Washington, D.C.

Nandra, K., Pounds, A.A.: 1994, MNRAS, 268, 405

Otto, A: 1990, Comp. Phys. Com. 59, 185

Otto, A., Birk, G.T.: 1993, Geophys. Res. Lett. 20, 2833

Papadopoulos, K.: 1979, in Dynamics of the Magnetosphere, Ed. Akasofu, S.I., Reidel, Dordrecht

Perley, R.: 1989, in Hot Spots in Extragalactic Radio Sources, eds. K. Meisenheimer and H.J. Röser, Lecture Notes in Physics, Springer (Berlin), 1

Ruderman, M.A., Sutherland, P.G.: 1975, ApJ 196, 51

Sakai, J.-I., Ohsawa, Y.: 1987, Space Sci. Rev. 46, 113

Schindler, K.: 1991, Geophys. Astrophys. Fluid Dynamics 62, 37

Schindler, K., Hesse, M., Birn, J.: 1991, ApJ 380, 293

Schmutzler, T., Lesch, H.: 1989, A&A 223, 71

Spicer, D.S.: 1976, Solar Physics 53, 305

Standke, K.J., Quirrenbach, A., Krichbaum, T.P., et al.: 1996, A&A 306, 27

Stella, L., Rosner, R.: 1984, ApJ 277, 312

Straumann, N.: 1986 General Realtivity and Relativistic Astrophysics, Springer, Berlin

Svensson, R.: 1987, MNRAS 227, 403

Svensson, R.: 1990, in Physical Processes in Hot Cosmic Plasmas, eds. W. Brinkmann et al., Kluwer, Dordrecht, 357

Ulrich, M.-H.: 1991, in Structure and Emission Properties of Accretion Disks, IAU Colloq. 129, eds. C. Bertout, S. Collin-Souffrin, J.P. Lasota and J. Tran Than Van

Winske, D., Tanaka, M., Wu, C.S. et al.: 1985, JGR 90, 123

Zdiarski, A.A., Lightman, A.P., Maciolek-Niedzwecki, A.: 1993, ApJ 414, L93